

Scientific paper

# Relative Stability and Spectroscopic Regularity of $C_{80}O$ Based on $C_{80}(D_{5d})$

Haomiao Zhang,<sup>1,2</sup> Tanzhang Chen,<sup>2</sup> Yingying Yu<sup>2</sup> and Shi Wu<sup>1,\*</sup>

<sup>1</sup> Department of Chemistry, Zhejiang University, 310027 Hangzhou, China

<sup>2</sup> Department of Chemical Engineering & Bioengineering, Zhejiang University, 310027 Hangzhou, China

\* Corresponding author: E-mail: wushi@zju.edu.cn

Tel.: +86-57188206529

Received: 19-05-2010

## Abstract

The relative stabilities of the nine possible isomers for  $C_{80}O$  based on  $C_{80}(D_{5d})$  were investigated via density function theory (DFT) at B3LYP/6-31G(d) level. The most stable geometry of  $C_{80}O$  is predicted to be 23,24- $C_{80}O$ , where an annulene-like structure is formed. The stretching vibration frequencies of the C=C bonds in the IR spectrum of  $C_{80}O$  compared with those of the C=C bonds in the IR spectrum of  $C_{80}(D_{5d})$  are basically blue-shifted. The signals of the bridged carbon atoms in the NMR spectrum of  $C_{80}O$ , computed at B3LYP/6-31G level, are changed upfield compared with those of the corresponding carbon atoms in the NMR spectrum of  $C_{80}(D_{5d})$ . The anti-aromaticity of rings in  $C_{80}O$  relative to that of the corresponding rings in  $C_{80}(D_{5d})$  is decreased according to the NICS values at the dummy centers of these rings calculated at B3LYP/6-31G level. A hexagon in 21,22- $C_{80}O$  even shows a tendency of aromaticity.

**Keywords:**  $C_{80}O$ , B3LYP/6-31G(d), blue-shift,  $^{13}C$  NMR, NICS.

## 1. Introduction

The functionalization of fullerenes has been an interesting research field for recent years because the modified fullerenes can be widely used in medicine, pharmacy and material science. There are seven isomers of the fullerene cage  $C_{80}$  satisfying the isolated pentagon rule (IPR). These isomers are  $C_{80}(C_{2v})$ ,  $C_{80}(C_{2v'})$ ,  $C_{80}(D_2)$ ,  $C_{80}(D_3)$ ,  $C_{80}(D_{5d})$ ,  $C_{80}(D_{5h})$  and  $C_{80}(I_h)$ , respectively.  $C_{80}(D_2)$  and  $C_{80}(D_{5d})$  are predicted to be more stable than the other five isomers by using DFT.<sup>1</sup> Furthermore, the  $C_2$  fragmentation energy of  $C_{80}(D_{5d})$  is slightly higher than that of  $C_{80}(D_2)$ .<sup>2</sup> Despite this,  $C_{80}(D_{5d})$  has been synthesized and characterized, which owns the five unique carbon atoms.<sup>3</sup> For  $C_{80}(D_{5d})$  has also been proven to possess a typical structure with pyrene-like tetracycle moieties on the ellipsoidal cage,<sup>4</sup> which show a high reactivity.<sup>5,6</sup> The conjugation system of  $C_{80}(D_{5d})$  is able to accept extra electrons. When two electrons in the Ti atom of  $Ti_2@C_{80}(D_{5d})$  are transferred to the cage, the  $C_{80}^{4+}(D_{5d})$  can be formed.<sup>7</sup> The similar electron transfer occurs in  $Sc_2@C_{80}(D_{5d})$ . Thus the energy gap of  $Sc_2@C_{80}(D_{5d})$  compared to that of  $C_{80}(D_{5d})$  is reduced,<sup>8</sup> which is favorable to elevating the semi-conductivity of the material. The thermodynamic stability of

$C_{80}(D_{5d})$  can be improved by the endohedral doping with the Be, C, Si, or Ge atoms.<sup>9</sup> Simultaneously, the physical properties of  $C_{80}(D_{5d})$  like the magnetic moment can be changed by increasing the number of the  $Er^{3+}$  ions in  $Er-Sc_2N@C_{80}$ .<sup>10</sup> Besides the encapsulation inside the cage, the exohedral chemical functionalization on the cage also alters the characters of  $C_{80}(D_{5d})$ . The addition of methylamine onto the  $C_{80}$  cage is predicted to solve a low solubility problem of the fullerenes in water.<sup>11</sup>

Although  $C_{80}O$  has been studied theoretically,<sup>12</sup> the  $C_{80}$  cage with the  $I_h$  symmetry is emphasized. Herein, more efforts are concentrated to the binding features of  $C_{80}(D_{5d})$ . First, the nine possible geometries of  $C_{80}O$  based on  $C_{80}(D_{5d})$  are studied to find the most stable geometry of  $C_{80}O$ . Then, the electronic structure and spectroscopic property of  $C_{80}O$  are investigated. Finally, the aromaticity of rings on the  $C_{80}O$  cage is explored.

## 2. Research Approach

Godly has recommended the IUPAC rule for the fullerenes.<sup>13</sup> According to this rule, the numbering system of  $C_{80}(D_{5d})$  was established as illustrated in Figure 1. The fi-

ve unique carbon atoms in  $C_{80}(D_{5d})$  were named as C(I), C(II), C(III), C(IV) and C(V). Also, nine kinds of bonds in  $C_{80}(D_{5d})$  were defined as the bonds a, b, c, d, e, f, g, h and i. On the basis of the geometry of  $C_{80}(D_{5d})$ , an oxygen atom was added to the nine kinds of bonds, and thus nine isomers of  $C_{80}O$  were designed. These isomers were 1,2- $C_{80}O$ , 1,9- $C_{80}O$ , 6,7- $C_{80}O$ , 7,8- $C_{80}O$ , 7,22- $C_{80}O$ , 21,22- $C_{80}O$ , 22,23- $C_{80}O$ , 23,24- $C_{80}O$  and 23,42- $C_{80}O$ , respectively. In the isomer 1,2- $C_{80}O$ , 1,2- stands for the bond added by the oxygen atom.

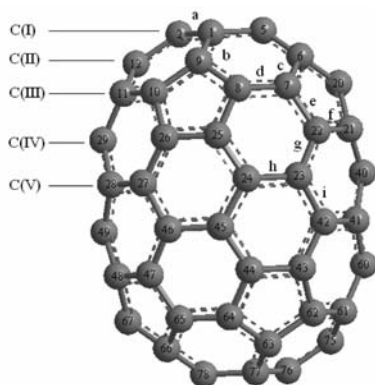


**Fig. 1.** The optimized geometry of  $C_{80}(D_{5d})$  at B3LYP/6-31G(d) level.

Full geometric optimization without any symmetric restriction for these nine isomers of  $C_{80}O$  was firstly performed using PM3 method. Further optimization of these isomers was carried out employing Becke three parameters plus Lee, Yang and Parr's (B3LYP) method<sup>14</sup> with the STO-3G, 3-21G and 6-31G(d) basis sets in density function theory (DFT), step by step, in order to save computation time. These methods, in Gaussian 03 program package,<sup>15</sup> have been used to study electronic structures of the supramolecular complexes,<sup>16</sup> fluorescent materials,<sup>17</sup> fullerenes,<sup>18</sup> and other compounds.<sup>19</sup> Then the equilibrium geometries with the minimum energies of the  $C_{80}O$  isomers were obtained. According to Koopmans' theory, vertical ionization potential (IP) is approximately defined as the negative value of HOMO (the highest occupied molecular orbital) energy. Similarly, vertical electron affinity (EA) is defined as the negative value of LUMO (the lowest unoccupied molecular orbital) energy. Absolute hardness ( $\eta$ ) is equal to the half of the difference between IP and EA. Absolute electron negativity ( $\chi$ ) is defined as the half of the sum for IP and EA. All these variables were calculated at B3LYP/6-31G(d) level.

Based on the B3LYP/6-31G(d) geometry optimized  $C_{80}O$  isomers, the IR spectra of the  $C_{80}O$  isomers were calculated using PM3 method. The  $^{13}C$  NMR spectra and NICS (nucleus independent chemical shift) values of rings in the  $C_{80}O$  isomers were investigated at B3LYP/6-

31G level using GIAO (gauge-including atomic orbital) method.<sup>20</sup> The NICS values of the several hexagons and pentagons in the stable  $C_{80}O$  isomers were studied by using a dummy center of the ring on the cage. These NICS values were used to measure the aromaticity of the rings, which was proposed by P. v. R. Schleyer *et al.*<sup>21</sup>

## 3. Results and Discussion

### 3.1. Relative Energies at B3LYP/6-31G(d) Level

The optimized results of  $C_{80}(D_{5d})$  were compared with the experimental values and other calculation results. The lengths of the nine kinds of bonds a–i in  $C_{80}(D_{5d})$  optimized at B3LYP/6-31G(d) level are 0.146, 0.139, 0.145, 0.140, 0.143, 0.147, 0.140, 0.146 and 0.146 nm, respectively. The bond lengths in  $C_{80}(D_{5d})$ , calculated by using RHF/STO-3G method are within the range of 0.136–0.147 nm,<sup>5</sup> which supports our results. The length and width of the  $C_{80}(D_{5d})$  cage are 0.914 and 0.705 nm, respectively, and they are in agreement with other calculated results; namely 0.946 and 0.716 nm, respectively.<sup>22</sup> The ratio between the long and short axes of  $C_{80}(D_{5d})$  is 1.296, which is compatible with the experimental value 1.3.<sup>3</sup>

The most stable geometries of  $C_{80}O$  are found to be 23,24- $C_{80}O$  and 21,22- $C_{80}O$ . The total energy of 23,24- $C_{80}O$  optimized at B3LYP/6-31G(d) level of theory is -84997.879 eV. The relative energy of 23,24- $C_{80}O$  is the lowest among the nine isomers of  $C_{80}O$  (Table 1), thus 23,24- $C_{80}O$  is the most stable isomer thermodynamically. While the relative energy of 21,22- $C_{80}O$  is 0.310 eV higher than in 23,24- $C_{80}O$ , the 21,22- $C_{80}O$  can be listed as the second most stable isomer of the nine isomers of  $C_{80}O$ .

The former stability order can be explained by the position of the added oxygen atom, which is located near the equatorial belt of  $C_{80}(D_{5d})$ . This position is preferable because of the lengths of the C(23)-C(24) and C(21)-C(22) bonds in  $C_{80}(D_{5d})$ , 0.146 and 0.147 nm, respectively, which are relatively long. These weak bonds can be easily broken when the oxygen atom approaches, and then the annulene-like open structures are formed in 23,24- $C_{80}O$  and 21,22- $C_{80}O$ . The formation of the annulene-like structure is favorable for reducing the tension of rings in the cage. At last, 23,24- $C_{80}O$  and 21,22- $C_{80}O$  own the  $C_s$  symmetry. Thereby, 23,24- $C_{80}O$  and 21,22- $C_{80}O$  are stable isomers.

The third stable isomer of  $C_{80}O$  is 1,2- $C_{80}O$  with  $C_s$  symmetry. The length 0.146 nm of the bond C(1)–C(2) in  $C_{80}(D_{5d})$  before the addition of the oxygen atom is long and weak; thus the annulene-like structure is formed in 1,2- $C_{80}O$ . But the bond C(1)–C(2) is located near the pole of  $C_{80}(D_{5d})$ , thus 1,2- $C_{80}O$  is less stable than the former two isomers of  $C_{80}O$ . The fourth stable isomer of  $C_{80}O$  is 1,9- $C_{80}O$  with the  $C_s$  symmetry. The bond C(1)–C(9) is

also located near the pole of  $C_{80}(D_{5d})$ . Whereas the length 0.139 nm of the bond C(1)–C(9) in  $C_{80}(D_{5d})$  before the addition of the oxygen atom is short and strong, thus the epoxy structure is formed in 1,9- $C_{80}O$ . Therefore, 1,9- $C_{80}O$  is less stable than 1,2- $C_{80}O$ .

6,7- $C_{80}O$ , 22,23- $C_{80}O$ , 7,22- $C_{80}O$  and 23,42- $C_{80}O$  without any symmetry are less stable than the former four isomers of  $C_{80}O$ . The length 0.146 nm of the bond C(23)–C(42) in  $C_{80}(D_{5d})$  before the addition of the oxygen atom is long, and the annulene-like structure is formed in 23,42- $C_{80}O$ , which is near the equatorial belt of  $C_{80}(D_{5d})$ . In spite of these, 23,42- $C_{80}O$  possesses no symmetry, thus it is the most unstable isomer of  $C_{80}O$ . Although 7,8- $C_{80}O$  displays the  $C_s$  symmetry, it is less stable than the former four isomers of  $C_{80}O$ . The length 0.140 nm of the bond C(7)–C(8) in  $C_{80}(D_{5d})$  before the addition of the oxygen atom is short, thus the epoxy structure is formed in 7,8- $C_{80}O$ .

0.688 eV computed by using RHF/STO-3G method.<sup>5</sup> The energies of HOMO and LUMO of 23,24- $C_{80}O$  are –5.022 and –3.977 eV. The energy gap of 23,24- $C_{80}O$  is 1.045 eV, which is higher than 0.988 eV of  $C_{80}(D_{5d})$ . The energy gaps of 21,22- $C_{80}O$ , 1,2- $C_{80}O$ , and 1,9- $C_{80}O$  are 1.194, 0.999, and 1.020 eV, respectively, which are also higher than that of  $C_{80}(D_{5d})$ . As a consequence, the kinetic stability of the stable  $C_{80}O$  isomers to the excitation of electrons in HOMO increases in contrast to that of  $C_{80}(D_{5d})$ .

The IP, EA,  $\eta$ , and  $\chi$  values of  $C_{80}(D_{5d})$  are 4.941, 3.953, 0.494, and 4.447 eV, respectively. The IP values of the  $C_{80}O$  isomers except 7,8- $C_{80}O$  are higher than that of  $C_{80}(D_{5d})$ . Then these  $C_{80}O$  isomers are unlikely to lose the electrons in HOMOs in the presence of the oxygen atom. The EA values of the  $C_{80}O$  isomers except 21,22- $C_{80}O$  and 22,23- $C_{80}O$  are higher than that of  $C_{80}(D_{5d})$ . Thus most of the  $C_{80}O$  isomers are ready to accept the electrons in LUMOs. The  $\eta$  values of the  $C_{80}O$  isomers except

**Table 1.** Relative energies ( $E_r$ ) and some parameters (eV) of  $C_{80}O$  isomers at B3LYP/6-31G(d) level

Compounds	$E_r$	$E_{\text{HOMO}}$	$E_{\text{LUMO}}$	$E_g$	IP	EA	$\eta$	$\chi$
23,24- $C_{80}O$	0	–5.022	–3.977	1.045	5.022	3.977	0.522	4.500
21,22- $C_{80}O$	0.310	–5.083	–3.890	1.194	5.083	3.890	0.597	4.487
1,2- $C_{80}O$	0.467	–4.959	–3.959	0.999	4.959	3.959	0.500	4.459
1,9- $C_{80}O$	0.516	–4.990	–3.969	1.020	4.990	3.969	0.510	4.479
6,7- $C_{80}O$	0.554	–4.984	–3.985	0.998	4.984	3.985	0.499	4.485
7,8- $C_{80}O$	0.812	–4.920	–4.029	0.891	4.920	4.029	0.445	4.474
22,23- $C_{80}O$	0.909	–5.120	–3.923	1.198	5.120	3.923	0.599	4.522
7,22- $C_{80}O$	1.118	–5.143	–3.957	1.186	5.143	3.957	0.593	4.550
23,42- $C_{80}O$	1.405	–5.011	–3.971	1.040	5.011	3.971	0.520	4.491



**Fig. 2.** The optimized geometries of 23,24- $C_{80}O$  and 21,22- $C_{80}O$  at B3LYP/6-31G(d) level.

### 3. 2. Electronic Structures at the Ground State

The energy gap ( $E_g$ ) of  $C_{80}(D_{5d})$  is calculated to be 0.988 eV at B3LYP/6-31G(d) level, which is higher than

7,8- $C_{80}O$  are higher than that of  $C_{80}(D_{5d})$ . Then the  $C_{80}O$  isomers are basically more stable thermodynamically than  $C_{80}(D_{5d})$ . The  $\chi$  values of all the  $C_{80}O$  isomers are higher than that of  $C_{80}(D_{5d})$ . Thus, the  $C_{80}O$  isomers are oxidized with difficulty compared to  $C_{80}(D_{5d})$ .

### 3. 3. IR Spectra

The absorptions in the IR spectrum of a molecule are affected by the crystal field, thermal fluctuations and quantization of the nuclear motion.<sup>23,24</sup> Herein the absorptions in the IR spectrum of a single molecule for  $C_{80}(D_{5d})$  in vacuum were studied. There are several moderate bands within 500–1000  $cm^{-1}$ , weak bands within 1000–1400  $cm^{-1}$  and strong bands within 1400–1700  $cm^{-1}$  in the IR spectrum of  $C_{80}(D_{5d})$ . The main IR absorptions at 931.9, 1573.9 and 1709.8  $cm^{-1}$  of  $C_{80}(D_{5d})$  are ascribed to puckering vibrations of aryl rings, stretching vibrations of C–C bonds and stretching vibrations of C=C bonds.

The stretching vibrations of the C=C bonds in the IR spectra of the  $C_{80}O$  isomers with the annulene-like structure compared with those of the C=C bonds in the IR spectrum of  $C_{80}(D_{5d})$  are blue-shifted. The main IR absorptions at 1712.3, 1712.5, 1714.4, 1713.9, 1713.8 and 1727.5  $cm^{-1}$  of 1,2- $C_{80}O$ , 6,7- $C_{80}O$ , 7,8- $C_{80}O$ , 7,22- $C_{80}O$ , 21,22- $C_{80}O$  and 23,42- $C_{80}O$  compared with the IR absorption at 1709.8  $cm^{-1}$  of  $C_{80}(D_{5d})$  are blue-shifted. The Mulliken charge of the oxygen atom in  $C_{80}O$  is negative. For example, the Mulliken charge of the oxygen atom in 1,2- $C_{80}O$  is -0.519. Since the electrons in  $C_{80}O$  are attracted from the  $C_{80}$  cage to the oxygen atom, the electron density on the C=C bonds near the oxygen atom is elevated. Thus, these C=C bonds are strengthened. There are some other main absorptions within the range of 1000–1400  $cm^{-1}$  in the IR spectra of the  $C_{80}O$  isomers. These absorptions split compared to those of  $C_{80}(D_{5d})$ . The symmetry of  $C_{80}O$  is decreased owing to the addition of the oxygen atom.

### 3. 4. NMR Spectra

The solvent effect and quantum average play important roles in the investigation on signals of the carbon atoms in the NMR spectrum of a molecule.<sup>25</sup> Herein the anisotropic signals of the carbon atoms in the NMR spectrum of a single molecule for  $C_{80}(D_{5d})$  in vacuum were studied. The  $^{13}C$  signals of the five unique carbon atoms in  $C_{80}(D_{5d})$  are 151.7, 164.6, 164.0, 125.2 and 156.6 ppm, which are basically identical to the experimental values 156.3, 163.9, 152.4, 128.9 and 130.2 ppm, respectively.<sup>3</sup> The  $^{13}C$  signals of 23,24- $C_{80}O$  are located within the range of 111.3–172.5 ppm (Figure 3), which are caused by the  $sp^2$ -C atoms on the cage. This range is wider than the range of 125.2–164.6 ppm for  $C_{80}(D_{5d})$ . Also, more signals in the NMR spectrum of 23,24- $C_{80}O$  are produced than those in the NMR spectrum of  $C_{80}(D_{5d})$ . These results are attributed to the decrease in symmetry of 23,24- $C_{80}O$  compared to that of  $C_{80}(D_{5d})$ . The signals at 119.9 ppm of the bridged carbon atoms C(23) and C(24) in 23,24- $C_{80}O$ , compared with the signal at 156.6 ppm of the corresponding carbon atoms in  $C_{80}(D_{5d})$ , are changed upfield. The electron density on these carbon atoms is increased owing to the strong electron-withdrawing effect

of the oxygen atom, thus the shielding effect is intensified. Actually, the signals at 111.3, 111.3, 120.6, 154.7, 153.0, and 122.8 ppm of the nearby carbon atoms C(22), C(25), C(26), C(27), C(28), and C(29) with the reference to 125.2, 125.2, 125.2, 156.6, 156.6, and 125.2 ppm of the corresponding carbon atoms in  $C_{80}(D_{5d})$  are all transferred upfield. The range of the  $^{13}C$  signals in 21,22- $C_{80}O$  is 125.5–189.7 ppm, which is also wider than that of the  $^{13}C$  signals in  $C_{80}(D_{5d})$ . More  $^{13}C$  signals in 21,22- $C_{80}O$  than those in  $C_{80}(D_{5d})$  are produced.

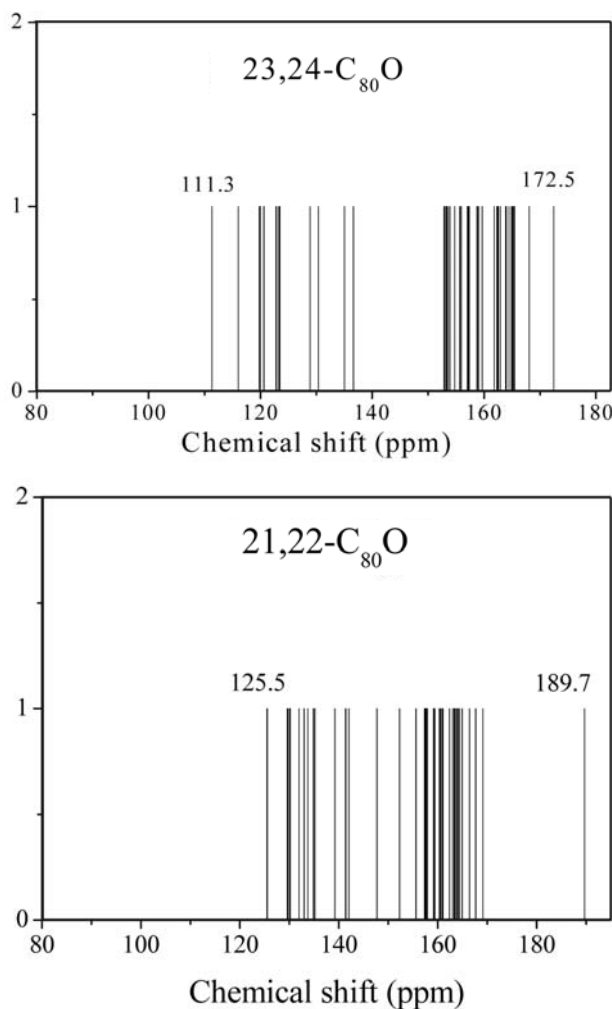


Fig. 3. The  $^{13}C$  NMR spectra of 23,24- $C_{80}O$  and 21,22- $C_{80}O$  isomers at B3LYP/6-31G level.

The signals of the bridged carbon atoms in 1,2- $C_{80}O$  with the annulene-like structure are located at 105.8 and 104.5 ppm, which are moved upfield relative to 151.7 and 151.7 ppm of the corresponding carbon atoms in  $C_{80}(D_{5d})$ . The signals at 148.0 and 147.9 ppm of the bridged carbon atoms in 6,7- $C_{80}O$  with the annulene-like structure are also transferred upfield relative to 164.6 and 164.0 ppm of the corresponding carbon atoms in  $C_{80}(D_{5d})$ .

The signals of the bridged carbon atoms in 1,9- $C_{80}O$  with the epoxy structure are situated at 82.6 and 93.1 ppm, which are changed upfield relative to 151.7 and 164.6 ppm of the corresponding carbon atoms in  $C_{80}(D_{5d})$ . The signals at 99.1 ppm of the bridged carbon atoms in 7,8- $C_{80}O$  with the epoxy structure relative to 164.0 ppm of the corresponding carbon atoms in  $C_{80}(D_{5d})$  are changed upfield. The signals at 70.9 and 65.1 ppm of the bridged carbon atoms in 7,22- $C_{80}O$  with the epoxy structure relative to 164.0 and 125.2 ppm of the corresponding carbon atoms in  $C_{80}(D_{5d})$  are also changed upfield. The signals at 90.2 and 74.3 ppm in 22,23- $C_{80}O$  with the epoxy structure relative to 125.2 and 156.6 ppm of the corresponding carbon atoms in  $C_{80}(D_{5d})$  are changed upfield as well. These are caused by the formation of the  $sp^3-C$  atoms in the epoxy structure of the above  $C_{80}O$  isomers.

### 3. 5. Aromaticity

The NICS value is the negative value of the absolute magnetic shielding effect calculated using a dummy centre in an aromatic system. There are five kinds of rings in  $C_{80}(D_{5d})$ , which are determined by the five unique carbon atoms. Of these rings, three kinds of hexagons are marked with I, II and III, respectively; and two kinds of pentagons are signed with IV and V. The NICS values at the dummy centre of rings I–V in  $C_{80}(D_{5d})$  are positive (Figure 4), thus these rings possess the anti-aromaticity. At the same time, there exists an apparent inhomogeneity of the magnetic field produced by  $\pi$  electrons on the  $C_{80}(D_{5d})$  cage. The NICS values of the pentagons are higher than those of the hexagons, thus the anti-aromaticity of the pentagons is stronger than that of the hexagons. This is because the conjugation effect in the pentagons is not as good as that in the hexagons. The NICS value of ring III is the highest of all the three hexagons, thus ring III exhibits the strongest

anti-aromaticity. The strong anti-aromaticity generally results in the high reactivity; therefore, ring III is the most reactive site of all the hexagons in  $C_{80}(D_{5d})$ , which is exactly located on the equatorial belt of the cage.

The NICS values at the dummy centre of rings I–V in 23,24- $C_{80}O$  are positive, and thus these rings are also anti-aromatic. The NICS values of rings I, III, IV and V in 23,24- $C_{80}O$  are decreased compared with those of the same rings in  $C_{80}(D_{5d})$ , respectively. Thus the anti-aromaticity of these rings is weakened. The presence of the oxygen atom is favourable to depressing the anti-aromaticity of these rings. The strong electronegativity of the oxygen atom increases the electron density and thus elevates the shielding effect of these rings. The NICS values of rings II, III, IV and V in 21,22- $C_{80}O$  in view of those of the corresponding rings in  $C_{80}(D_{5d})$  are depressed, thus the anti-aromaticity of these rings is reduced. Especially, the NICS value of ring II is negative, thus ring II displays a tendency of the aromaticity owing to the addition of the oxygen atom.

### 4. Conclusions

In summary, the most stable isomer of  $C_{80}O$  was predicted to be 23,24- $C_{80}O$  with  $C_s$  symmetry. The bond C(23)–C(24) added by the oxygen atom is located near the equatorial belt of  $C_{80}(D_{5d})$ . This bond is weak, thus the annulene-like structure is formed in 23,24- $C_{80}O$ . The signals of the bridged carbon atoms in the NMR spectrum of  $C_{80}O$  are changed upfield relative to those of the corresponding carbon atoms in the NMR spectrum of  $C_{80}(D_{5d})$ . The anti-aromaticity of the rings in 23,24- $C_{80}O$  and 21,22- $C_{80}O$  is decreased compared with that of the corresponding rings in  $C_{80}(D_{5d})$ . Therefore, the kinetic stability of the  $C_{80}(D_{5d})$  cage can be improved upon the addition of the oxygen atom.

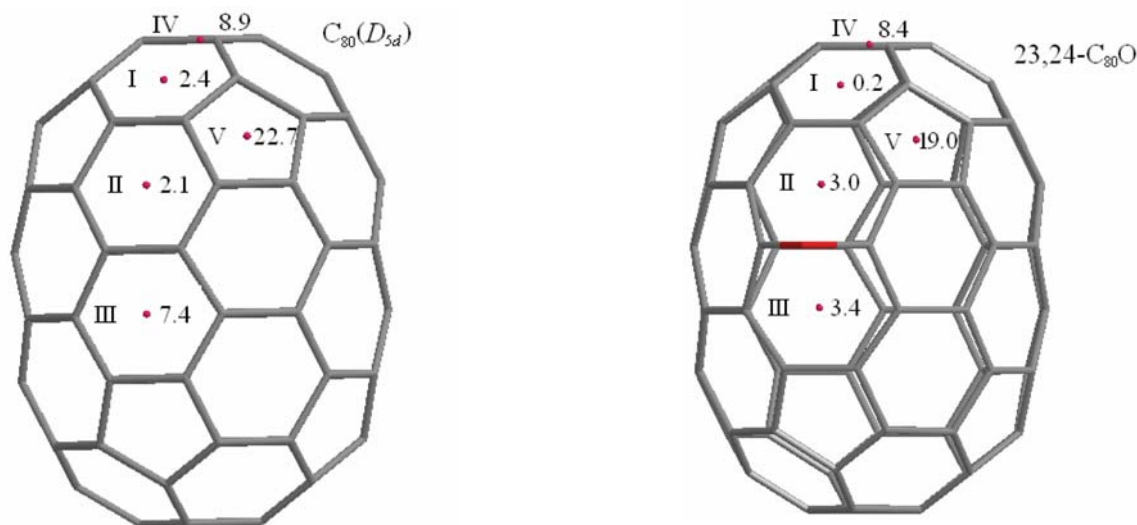


Fig. 4. The NICS values of the given rings in  $C_{80}(D_{5d})$  and 23,24- $C_{80}O$  at B3LYP/6-31G level.

## 5. Acknowledgements

We are very grateful to Prof. Jikang Feng at Jilin University for providing ZINDO program.

## 6. References

1. G. Sun, M. Kertesz, *Chem. Phys. Lett.* **2000**, *328*, 387–395.
2. G. A. Dolgonos, G. H. Peslherbe, *Chem. Phys. Lett.* **2004**, *398*, 217–223.
3. C. R. Wang, T. Sugai, T. Kai, T. Tomiyama, H. Shinohara, *Chem. Commun.* **2000**, 557–558.
4. Y. Sato, K. Suenaga, S. Okubo, T. Okazaki, S. Iijima, *Nano Lett.* **2007**, *7*, 3704–3708.
5. X. Wen, X. Ren, S. Wu, *Acta Chim. Slov.* **2008**, *55*, 419–424.
6. Y. Ding, P. Gao, L. Qin, Q. Teng, *Int. J. Quantum Chem.* **2009**, *109*, 693–700.
7. A. N. Enyashin, Yu. N. Makurin, A. L. Ivanovskii, *Comput. Mat. Sci.* **2006**, *36*, 26–29.
8. C. R. Wang, L. H. Gan, C. L. Bai, H. Shinohara, *China Particology* **2004**, *2*, 189–191.
9. L. Türker, *J. Mol. Struct.: Theochem* **2003**, *626*, 203–207.
10. A. Tiwari, G. Dantelle, K. Porfyakis, A. A. R. Watt, A. Ardavan, G. A. D. Briggs, *Chem. Phys. Lett.* **2008**, *466*, 155–158.
11. O. Amelines-Sarria, V. A. Basiuk, *Superlatt. Microstruct.* **2009**, *46*, 302–305.
12. M. Ibrahim, *Acta Chim. Slov.* **2005**, *52*, 153–158.
13. E. W. Godly, R. Taylor, *Pure Appl. Chem.* **1997**, *69*, 1411–1434.
14. (a) A. D. Becke, *J. Chem. Phys.* **1993**, *98*, 5648–5652. (b) C. Lee, W. Yang, R. G. Parr, *Phys. Rev. B* **1988**, *37*, 785–789.
15. M. J. Frisch, G. W. Trucks, H. B. Schlegel, G. E. Scuseria, M. A. Robb, J. R. Cheeseman, J. A. Montgomery, T. Vreven Jr., K. N. Kudin, J. C. Burant, J. M. Millam, S. S. Iyengar, J. Tomasi, V. Barone, B. Mennucci, M. Cossi, G. Scalmani, N. Rega, G. A. Petersson, H. Nakatsuji, M. Hada, M. Ehara, K. Toyota, R. Fukuda, J. Hasegawa, M. Ishida, T. Nakajima, Y. Honda, O. Kitao, H. Nakai, M. Klene, X. Li, J. E. Knox, H. P. Hratchian, J. B. Cross, C. Adamo, J. Jaramillo, R. Gomperts, R. E. Stratmann, O. Yazyev, A. J. Austin, R. Cammi, C. Pomelli, J. W. Ochterski, P. Y. Ayala, K. Morokuma, G. A. Voth, P. Salvador, J. J. Dannenberg, V. G. Zakrzewski, S. Dapprich, A. D. Daniels, M. C. Strain, O. Farkas, D. K. Mallick, A. D. Rabuck, K. Raghavachari, J. B. Foresman, J. V. Ortiz, Q. Cui, A. G. Baboul, S. Clifford, J. Cioslowski, B. B. Stefanov, G. Liu, A. Liashenko, P. Piskorz, I. Komaromi, R. L. Martin, D. J. Fox, T. Keith, M. A. Al-Laham, C. Y. Peng, A. Nanayakkara, M. Challacombe, P. M. W. Gill, B. Johnson, W. Chen, M. W. Wong, C. Gonzalez, J. A. Pople, *Gaussian 03, Revision B. 01*, Gaussian Inc., Pittsburgh, PA, **2003**.
16. (a) V. M. Leovač, S. Marković, V. Divjaković, K. M. Szécsényi, M. D. Joksović, I. Leban, *Acta Chim. Slov.* **2008**, *55*, 850–860. (b) V. B. Delchev, M. V. Nenkova, *Acta Chim. Slov.* **2008**, *55*, 132–137. (c) L. Türker, S. Gümüş, *Acta Chim. Slov.* **2009**, *56*, 246–253. (d) V. V. Šukalović, M. V. Zlatović, G. M. Roglič, S. V. Kostić-Rajačić, D. B. Andrić, *Acta Chim. Slov.* **2009**, *56*, 270–277. (e) B. G. de Oliveira, M. L. A. de A. Vasconcellos, *Acta Chim. Slov.* **2009**, *56*, 340–344.
17. H. Zhao, J. Zhou, L. Hu, Q. Teng, *Chinese J. Chem.* **2009**, *27*, 1687–1691.
18. H. Sun, X. Yun, S. Wu, Q. Teng, *J. Mol. Struct.: Theochem* **2008**, *868*, 71–77.
19. (a) L. Türker, T. Atalar, *Acta Chim. Slov.* **2008**, *55*, 146–153. (b) R. Abbasoglu, A. Magerramov, Y. Asamaz, *Acta Chim. Slov.* **2009**, *56*, 237–245.
20. K. Wolinski, J. G. Hinton, P. Pulay, *J. Am. Chem. Soc.* **1990**, *112*, 8251–8260.
21. (a) P. v. R. Schleyer, C. Maerker, A. Dransfeld, H. Jiao, N. J. R. v. E. Hommes, *J. Am. Chem. Soc.* **1996**, *118*, 6317–6318. (b) P. v. R. Schleyer, H. Jiao, N. J. R. v. E. Hommes, V. G. Malkin, O. L. Malkina, *J. Am. Chem. Soc.* **1997**, *119*, 12669–12670. (c) P. v. R. Schleyer, M. Manoharan, Z. X. Wang, B. Kiran, H. Jiao, R. Puchta, N. J. R. v. E. Hommes, *Org. Lett.* **2001**, *3*, 2465–2468. (d) Z. Chen, C. S. Wannere, C. Corminboeuf, R. Puchta, P. v. R. Schleyer, *Chem. Rev.* **2005**, *105*, 3842–3888. (e) F. B. Shaidaei, C. S. Wannere, C. Corminboeuf, R. Puchta, P. v. R. Schleyer, *Org. Lett.* **2006**, *8*, 863–866. (f) Z. Chen, R. B. King, *Chem. Rev.* **2005**, *105*, 3613–3642.
22. K. Nakao, N. Kurita, M. Fujita, *Phys. Rev. B* **1994**, *49*, 11415–11420.
23. A. Jezierska, J. J. Panek, A. Koll, J. Mavri, *J. Chem. Phys.* **2007**, *126*, 205101–205109.
24. G. Pirc, J. Stare, J. Mavri, *J. Chem. Phys.* **2010**, *132*, 224506–224512.
25. J. Stare, A. Jezierska, G. Ambrozic, I. J. Kosir, J. Kidric, A. Koll, J. Mavri, D. Hadzi, *J. Am. Chem. Soc.* **2004**, *126*, 4437–4443.

## Povzetek

S pomočjo teorije gostotnih funkcionalov (DFT) na nivoju B3LYP/6-31G(d) so bile raziskane ravnotežne geometrijske strukture in relativne stabilnosti devetih možnih izomernih oblik  $C_{80}O$ , ki temeljijo na strukturi  $C_{80}(D_{5d})$ . Najbolj stabilna napovedana geometrija za  $C_{80}O$  je anulenu podobna struktura, 23,24- $C_{80}O$ , katere vezavno mesto je vez 6/6 blizu ekvatorialnega pasu molekule  $C_{80}(D_{5d})$ . Prvi absorpcijski vrh pri 634.1 nm v elektronskem spektru 23,24- $C_{80}O$  je relativno z elektronskim spektrom  $C_{80}(D_{5d})$  pomaknjen v bolj modro območje spektra. Najmočnejši IR vrh molekule  $C_{80}O$  je v primerjavi z vrhom  $C_{80}(D_{5d})$  pomaknjen v bolj rdeče območje spektra. Kemijski premiki v  $^{13}C$  so za mostovne ogljikove atome v epoksidnih strukturah  $C_{80}O$  glede na premike v anulenu podobnih strukturah pomaknjeni v višje polje. Anti-aromatičnost nekaterih heksagonov in pentagonov s površine kletke, ki tvori  $C_{80}O$ , pada v skladu z izračunanimi NICS vrednostmi ustreznih heksagonov in pentagonov v  $C_{80}(D_{5d})$ .